ESTIMATION OF THE DYNAMIC STABILITY OF A SLOPE DURING STRONG EARTHQUAKE MOTION

K. Toki (I), F. Miura (II) and Y. Oguni (III)
Presenting Author: K. Toki

SUMMARY

The stability of an existing slope during strong earthquake motion was investigated in detail by the nonlinear finite element technique. Joint elements were arranged for every interface between the soil elements. This proposed method showed sliding and separation phenomena of the progressive failure of a slope. The safety factor for the failure of a slope basically depends on the predominant frequency as well as the exciting acceleration amplitude. A large safety factor was estimated when the material nonlinearity was introduced even though the larger deformation of soil was calculated.

INTRODUCTION

We have proposed a general method for the analysis of problems of nonlinear dynamic soil structure interaction using the finite element method (Refs.1 and 2), in which the joint elements (Ref.3) represented the sliding and separation phenomena that exists between the structure and the soil. One of us used this analysis method to examine the stability of an existing slope during critical states. We here report the stability of this same slope based on quantitative detailed investigations that examined the material nonlinearity of its soil.

ANALYSIS PROCEDURE AND THE SLOPE INVESTIGATED

An analysis of slope stability usually is made by the sliding circle or by Bishop's and Junbu's method, the choice of method depending on the shape of the sliding surface (Ref.4). Although both are valid method for calculating static force, slope stability under dynamic forces can not be rationally estimated by these classical methods. The finite element method, however, makes it possible to estimate the dynamic stability of a slope during an earthquake; also the safety factor against the sliding of the slope, in particular, can be estimated directly by adopting joint elements set along an arbitrary sliding surface.

Joint elements were arranged not along a specified sliding surface but at every interfaces between all the soil elements as shown in Fig.1, consequently, each soil element (soil mass) is able to move in parallel to, perpendicular to and rotationally to all the others. This means that they express the kind of sliding and separation phenomena that occurs in an actual slope failure.

Based on earlier experimental results (Ref.5), the constitutive relation-

---

(I) Professor, Disaster Prevention Research Inst., Kyoto Univ., JAPAN
(II) Assoc. Professor, Fuculty of Eng., Yamaguchi Univ., Yamaguchi, JAPAN
(III) Engineer, Sumitomo Metal Industries Ltd., Wakayama, JAPAN

ships were assumed to be those shown in Figs.2(a) and (b) for the normal and tangential components, respectively, as is the same in the previous papers (Refs.1 and 2).

Considering the simplicity of the treatment in our numerical analysis and its conformity with the constitutive relationships of the joint elements, soil is here regarded as an elasto-perfect plastic body. The Mohr-Coulomb failure law was adopted as the criterion of yield. This relationship is given by

$$\tau_y = C\cos\phi - \sigma_m \sin\phi$$
$$\sigma_m = (\sigma_1 + \sigma_2) / 2$$

in which, τ_y is the yield shear stress, c is the cohesion, ϕ the internal friction angle, and σ_1 and σ_2 the maximum and the minimum principal stresses.

The cross section of the actual slope analysed and the finite element mesh of the model slope are shown in Fig.3. The slope is composed of banking and weathered rock under the basal rock is slate. This was determined by boring tests. The shear and volumetric wave velocities of each layer were determined by seismic prospecting. The material constants obtained from laboratory tests are listed in Table 1. Joint elements were used at every interface between the soil elements as shown schematically in Fig.1. The solid, broken and irregular broken lines in Fig.3 indicate the sliding surfaces for which safety factors were calculated. These surfaces were decided with reference to those given in a previous report.

DEFINITION OF SAFETY FACTORS

Slope stability is discussed on the basis of the two safety factors defined below:

The local safety factor (LSF)

Sliding first occurs locally at some point in the slope, then it propagates and is accompanied by stress redistribution. Let τ_y and τ be the yield and mobilized shear stresses of a joint element. The local safety factor is defined as the minimum value of the ratio $|\tau_y/\tau|$ of all the elements.

The total safety factor (TSF)

The total safety factor indicates the safety against sliding of the entire area above the sliding surface under consideration. It is defined by

$$TSF = \left| \sum_{j=1}^{N} \tau_{yj} \cdot l_j \Big/ \sum_{j=1}^{N} \tau_y \cdot l_j \right|$$

in which, N is the number of joint elements forming the sliding surface and, τ_{yj} and τ_j represent the yield shear stress, the mobilized shear stress and l_j is the length of the joint element j.

Before dynamic stability analysis was made, static analyses were made by the finite element method and their results compared with those obtained from classical methods in order to check their compatibility. When safety against sliding was compared for Junb's and the finite element method, fairly good agreement was obtained; but, in general, the latter produced lower safety factors.

DYNAMIC BEHAVIOR OF A SLOPE DURING STRONG EARTHQUAKE GROUND MOTION

The slope was subjected to simultaneous horizontal and vertical excitations of the three different accelerograms shown in Table 2. Table 2 lists the maximum amplitudes and predominant frequencies of the original accelerograms for four analyses. The maximum response distribution for excitation in Case 1 is shown in Fig.4. Fig.4(a) shows the horizontal acceleration and (b) the horizontal displacement. The soil is assumed to be a linear elastic material. The response acceleration is amplified to more than 500gal on the horizontal surface around the center of the slope. In contrast, little amplification is found in the right-hand region. Maximum response values appear at, or close to, the area in which geometrical change is remarkable. Large displacement is present in the right-hand region, especially at the toe where there was only slight amplification of acceleration.

Figs.5(a)-(d) show joint elements which slide and/or separate at the time indicated in each figure for the exitation of Case 1. First, local sliding is initiated along the interface between the weathered and basal rock in the toe region. The sliding area develops upward from the toe region as time elapses. In addition, separation penetrates the slope from point A on the surface to point B at the base by 1.68sec, indicative of the possibility of the collapse of the slope in this area. At 1.72sec, joint element D-E separates and at that time all the elements along the E-F line slide. This means that Sliding surface 1 (line D-E-F) slides as a whole. Sliding surfaces 2 and 3 do not slide as a whole although local sliding takes place during the period between 1.66 and 1.72sec, which corresponds to one of the peak accelerations of the NS component. As seen above, our proposed method is able to describe the progressive failure process.

THE EFFECT OF THE PREDOMINANT FREQUENCY

Time histories of a safety factor whose minimum value is a TSF are shown in Fig.6 for Sliding surface 1. Fig.6(a) shows data for Case 1, (b) Case2, (c) Case 3 and (d) Case 4. Sliding is denoted by the symbol ↓. It occurred five times in Case 1 and twice in Case 4. In Case 1, slding continued over a period in the first three occurrences, but it was instantaneous in the last two. In Case 4, sliding took place twice and continued for a time. The sliding magnitudes of the first three events in Case 1 and of the two in Case 4 are greater than those of the last two events in Case 1 because the sliding magnitude basically depends on the duration time of sliding. Note that the predominant periods of the input accelerograms on those occasions when sliding continued were relatively long. No sliding of the entire Sliding surface 1 took place in Cases 2 and 3 nor in any case for Sliding surfaces 2 and 3.

TSFs are summarized in Table 3. The lowest TSF in Case 1 in all sliding surfaces is due to its having the largest input acceleration amplitude. The amplitude of horizontal acceleration in Cases 2, 3 and 4 are almost the same but the predominant frequencies differ. Therefore, the TSF differences are caused by differences in the predominant frequency of the input accelerograms. The largest TSFs were obtained in Case 3, which had the highest predominant frequency. The lowest TSFs were obtained in Case 4 which had the lowest predominant frequency. The lower the predominant frequency, the greater the tendency of the slope to slide, and slope stability mainly depends on the predominant frequency. When slope stability is in question,

attention must be paid to the frequency value as well as to the input acceleration amplitude. In the static method, the safety factor is evaluated only by the maximum acceleration or the seismic coefficient, but dynamic analyses uses the predominant frequency of the acceleration as well as its maximum value.

THE EFFECT OF THE MATERIAL'S NONLINEARITY

The nonlinearity of the soil material was introduced. Strength parameters, including cohesion and the angle of internal friction, are listed in Table 1. The maximum response distribution is shown in Fig.7. Fig.7(a) shows the horizontal acceleration and (b) the displacement. The maximum response acceleration is about 450 gal; the area of 400 gal and above is limited to the surface surrounding the center of the slope. As the maximum value in the linear ground model was about 530 gal, soil nonlinearity reduced the maximum value by about 15%. A comparison of Figs.4(c) and 7(c) indicates that the displacement is about 1.5 times greater than when the soil is a linear elastic material. This large deformation for nonlinear soil is due to residual displacement.

The sliding and/or separating elements and the yielding soil elements are shown in Fig.8. Yielding (shear failure) is almost always associated with the occurrence of sliding. The sliding and yielding zone develop upward from the toe area in the linear soil case. In comparison with Fig.5, the number of sliding and/or separating elements is small. This is attributable to energy dissipation due to the nonlinear behavior of the soil.

The TSFs for Case 1 are tabulated in Table 4. Although Sliding surface 1 slides as a whole in both types of soil, TSFs in nonlinear soil are 10% larger for Sliding surfaces 2 and 3. This implies that a TSF lower than the actual value is estimated when the soil is assumed to be a linear elastic material.

When these results are compared with those of static analyses, the critical seismic coefficient k_H is 0.21 (206 gal) for Sliding surface 3. This surface does not slide, but the TSF is greater than 1.0 in Table 4 even when as large an amplitude as 340 gal is applied. Sliding surface 1 is stable when the amplitude of excitation is 200 gal although the critical seismic coefficient is 0.18 (176 gal). Again, lower TSFs than must actually exist are found by static methods, and the difference be as much as 70% as in the case of Sliding surface 3.

COUNTERMEASURES TO IMPROVE SLOPE STABILITY

There are, at present, several measures used to improve slope stability; driving a wall of piles, construction of a retaining wall and draining away ground water. Sheetpiles were driven into our model slope as a countermeasure, then slope stability was evaluated for dynamic loads. The sheetpile is represented by the beam element, the arrangement of which is illustrated in Fig.1. Beam elements sandwiched between joint elements are denoted by thick, solid lines. A kind of sheetpile (YSP-II) was used in our analysis. A cross section of the sheetpile and its material constants per 1m length are given in Table 5. Locations of the sheetpiles are shown in Fig.9.

Joint elements during sliding and/or separation are shown in Fig.9. YSP-II sheetpiles were driven in at points A and B on a slope that had been subjected to reduced accelerograms (200 gal NS, 120 gal UD). In comparison with Case 2 in which sheet pile is not used, the number of joint elements which slide or separate is greatly reduced. The maximum bending moments and stresses obtained from the seismic coefficient method (k_H =0.2) and from seismic response analyses are shown in Table 6. For a sheetpile at point B, static stress is greater than the yield stress value, 3000kg/cm*cm, whereas the dynamic stress is just at the allowable stress level. Furthermore, this 2463kg/cm*cm value is instantaneous; hence, the sheetpile is considered safe.

The slope will remain stable if sheetpiles are driven in at points A and B and if the seismic excitation amplitude is 200gal or less. But, static analysis showed that the slope would not remain stable for a seismic coefficient of 0.2 because the stress exceeded the yield stress level. Thus, the sheetpile at point B would yield when the slope is subjected to ground motion with the intensities of the original El Centro accelerograms with a maximum horizontal acceleration of 340gal. Accordingly, an additional YSP-II sheetpile was driven into the slope at point C to reduce the seismic load upon the sheetpile at point B. The resulting stress was reduced below the allowable value.

CONCLUSIONS

The stability of the slope investigated was quantitatively assessed for dynamic forces. The nonlinear finite element technique was used for this purpose. The following was concluded.

(1) Our proposed method expressed the progressive failure of a slope subjected to seismic excitation.

(2) Safety factors basically depend on the predominant frequency as well as on the amplitude of the horizontal input accelerogram. The lower the predominant frequency, the lower the safety factor.

(3) The material nonlinearity of the soil decreased the response acceleration by 15% and increased the displacement. Higher safety factors of 5-8% were obtained in comparison to the factors found when the slope was assumed to be a linear elastic material.

(4) Although the critical seismic coefficient was 0.21 (206gal) for the entire slope to slide (Sliding surface 3), it did not slide even when as large an amplitude as 342gal was applied. The slope was stable for surficial local collapse in the steep region of the slope (Sliding surface 1) when the excitation amplitude was 200gal even though the critical seismic coefficient was 0.18 (176gal).

(5) Slope failure was reduced when sheetpiles were driven in. Sliding in the deep areas disappeared; it was seen only near the surface.

(6) The bending stresses of the sheetpiles driven into the slope had 10-20% larger values in the seismic coefficient method than in dynamic analyses.

This study was done with a computer program, 7S-II (Seismic Safety of Soil-Structure Systems against Sliding and Separation, the second version). 7S-II will be provided on request.

REFERENCES

1. Toki, K., T. Sato and F. Miura: Separation and sliding between soil and structure during strong ground motion, Int. J. Eathq. Eng. and Structural Dynamics, Vol.9, pp.263-277, 1981.
2. Toki, K. and F. Miura: Nonlinear seismic response analysis of soil-structure interaction system, Int. J. Earthq. Eng. and Structural Dynamics, Vol.11, pp.77-89, 1983.
3. Goodman, R.E.: Method of geological engineering in discontinuous rocks, West Publishing Company, Ch.8, pp.300-368, 1976.
4. Chowdhurt, R.N.: Slope analysis, Elsevier Scientific Publishing Company, Ch.1, 1978.
5. Miura, F.: Estimation of the dynamic stability of a rigid structure during strong earthquake motion, Proc. 6th Japan Eathq. Symp., pp.1785-1792, 1982.

Table 1 Material constants and strength parameters of the slope.

	Unit weight (t/m^3)	Shear wave velocity (m/sec)	Poisson's ratio	Cohesion (kg/cm^2)	Angle of internal friction
Banking	1.6	150	0.4	0.1	29°
Weathered rock	1.9	300	0.4	0.1	45°
Joint element	Normal spring constant Shear spring constant Cohesion Friction angle		3.0x10 t/m^3 3.0x10 t/m^3 0.1 kg/cm^2 25°,35°		

Table 2 Maximum acceleration and predominant frequency of excitation accelerograms for four cases.

	Case 1		Case 2		Case 3		Case 4	
Input acceleration	El Centro		El Centro		JPL		Hachinohe	
	NS	UD	NS	UD	S82E	UD	EW	UD
Maximum acceleration (gal)	342	206	200	120	208	126	203	96
Predominant frequency (Hz)	1.15	8.55	1.15	8.55	2.88	2.95	0.83	1.25

Table 3 TSFs of the three sliding surfaces in the four cases.

Case \ Sliding surface	1	2	3
1	Sliding (≦1.0)	1.150	1.057
2	1.017	1.384	1.244
3	1.125	1.508	1.308
4	Sliding (≦1.0)	1.298	1.149

Table 4 Effects of the nonlinearity of the soil on TSF.

Ground \ Sliding surface	1	2	3
Linear elestic (Case 1)	Sliding (≦1.0)	1.150	1.057
Nonlinear	Sliding (≦1.0)	1.251	1.111

Table 5 Sheetpile constants.

Area of section (cm^2)	153
Moment of inertia of area (cm^4)	8690
h (cm)	10.0
e (cm)	8.18

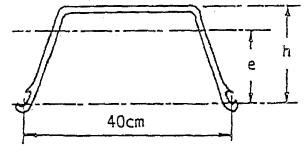

Table 6 Comparison of the bending moments and stresses from dynamic and static analyses.

	Bending moment (kg·cm/m)		Bending stress (kg/cm²)	
	Point A	Point B	Point A	Point B
Static	4.90×10^5	2.71×10^6	563.9	3120
Dynamic El Centro 200 gal	4.46×10^5	2.14×10^6	512.7	2463

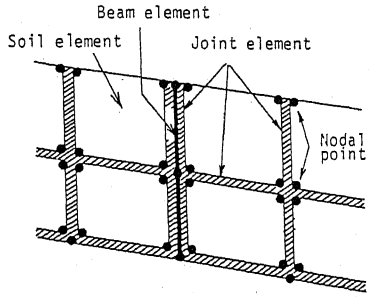

Fig.1 Discretization of the slope produced by solid, joint and beam elements.

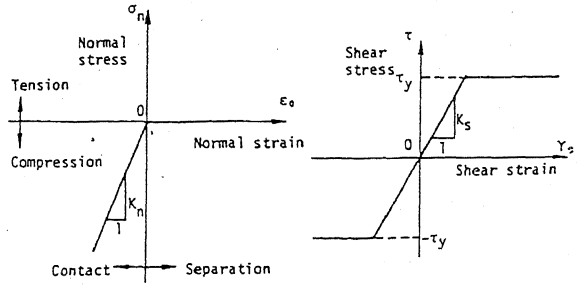

(a) Normal direction (b) Tangential direction

Fig.2 Constitutive relations of the joint element.

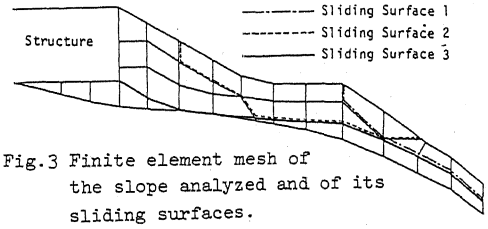

Fig.3 Finite element mesh of the slope analyzed and of its sliding surfaces.

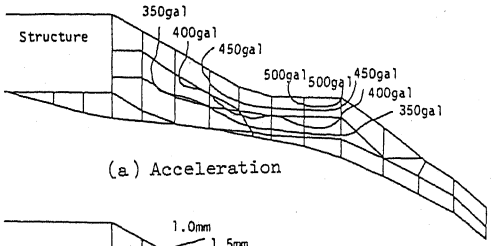

(a) Acceleration

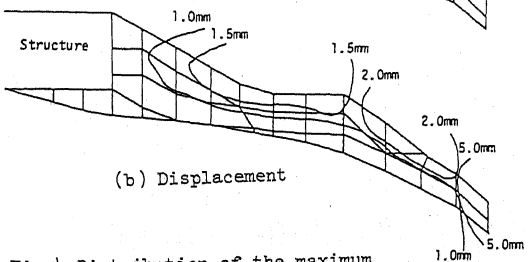

(b) Displacement

Fig.4 Distribution of the maximum horizontal responses (El Centro 342 gal).

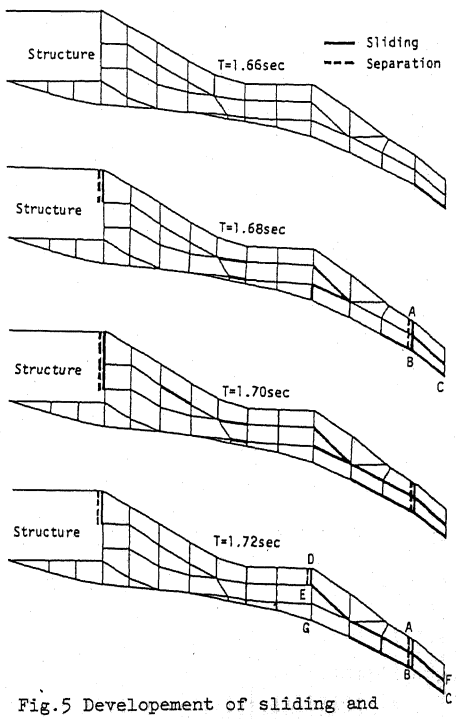

Fig.5 Developement of sliding and of the separating area with time.

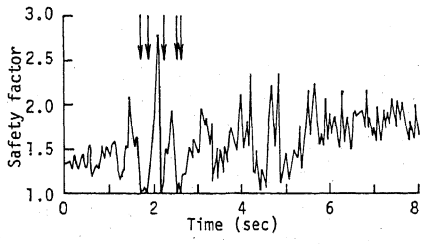

(a) Case 1

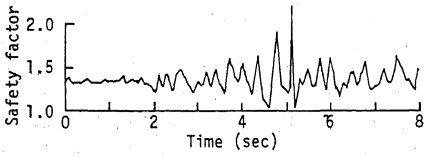

(b) Case 2

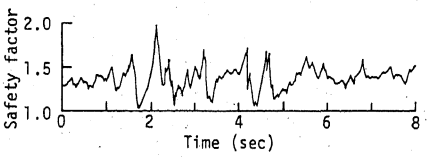

(c) Case 3

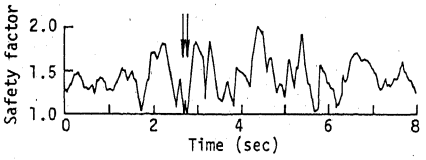

(d) Case 4

Fig.6 Time histories of the TSF for sliding surface 1.

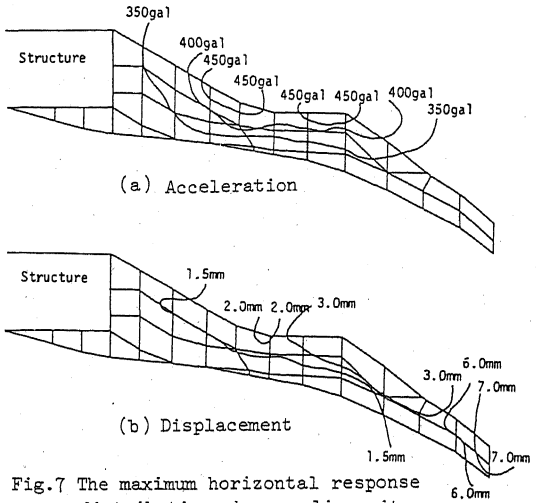

Fig.7 The maximum horizontal response distribution when nonlinearity of soil is taken into account(El Centro 342 gal).

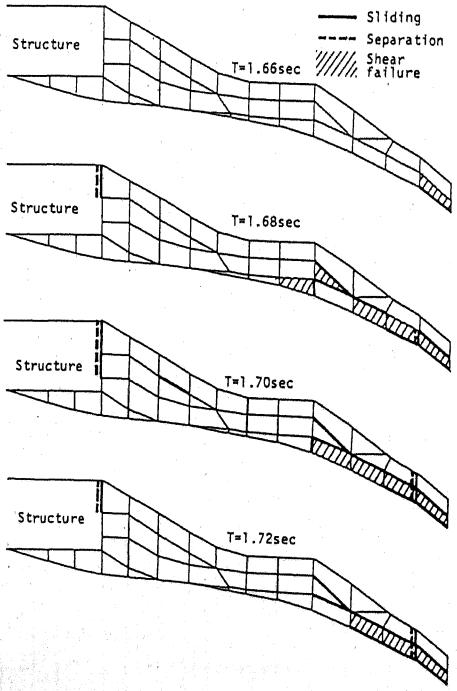

Fig.8 Development of the failure region with time.

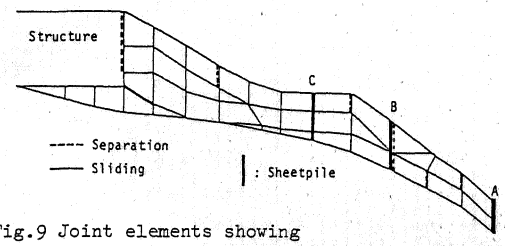

Fig.9 Joint elements showing separation and sliding when sheetpiles had been driven into points A and B.